ARTICLE

Quantum Dot Sensitized Solar Cells with Improved Efficiency Prepared Using Electrophoretic Deposition

Asaf Salant,[§,†] Menny Shalom,[§,‡] Idan Hod,[‡] Adam Faust,[†] Arie Zaban,[‡,*] and Uri Banin[†,*]

[†]Institute of Chemistry and the Center for Nanoscience and Nanotechnology, The Hebrew University, Jerusalem 91904, Israel, and [‡]Institute of Nanotechnology & Advanced Materials, Department of Chemistry, Bar-Ilan University, 52900 Ramat Gan, Israel. [§]These authors contributed equally to this work.

ABSTRACT Quantum dot sensitized solar cells (QDSSC) may benefit from the ability to tune the quantum dot optical properties and band gap through the manipulation of their size and composition. Moreover, the inorganic nanocrystals may provide increased stability compared to organic sensitizers. We report the facile fabrication of QDSSC by electrophoretic deposition of CdSe QDs onto conducting electrodes coated with mesoporous TiO_2. Unlike prior chemical linker-based methods, no pretreatment of the TiO_2 was needed, and deposition times as short as 2 h were sufficient for effective coating. Cross-sectional chemical analysis shows that the Cd content is nearly constant across the entire TiO_2 layer. The dependence of the deposition on size was studied and successfully applied to CdSe dots with diameters between 2.5 and 5.5 nm as well as larger CdSe quantum rods. The photovoltaic characteristics of the devices are greatly improved compared with those achieved for cells prepared with a linker approach, reaching efficiencies as high as 1.7%, under 1 sun illumination conditions, after treating the coated electrodes with ZnS. Notably, the absorbed photon to electron conversion efficiencies did not show a clear size-dependence indicating efficient electron injection even for the larger QD sizes. The electrophoretic deposition method can be easily expanded and applied for preparations of QDSSCs using diverse colloidal quantum dot and quantum rod materials for sensitization.

KEYWORDS: quantum dots · solar cells · electrophoretic deposition · quantum dot sensitized solar cell · size effects

Quantum dot sensitized solar cells[1−7] (QDSSC) employ the quantum dots as sensitizers, benefiting from the ability to tune the optical properties by controlling the QD size and composition.[8−10] In the QDSSC, the QDs are attached to a wide band gap semiconductor,[11−13] usually mesoporous TiO_2, in which, following light absorption, the electrons are injected, while the hole is transported *via* a suitable electrolyte to the counter-electrode. It has also been suggested that the stability may be improved by the use of inorganic sensitizers in the QDSSC.

QDSSCs have been fabricated using two fundamentally different approaches. The first and most common routes employ the *in situ* preparation of QDs onto the nanostructured wide bandgap semiconductor, either by chemical bath deposition[14−18] or by successive ionic layer adsorption and reaction.[19,20] These methods provide high surface coverage of QDs, with good anchoring to the electrodes, but the control over the QD size is limited and the size distribution is broad. This problem may be alleviated by fabricating QDSSCs with monodisperse QDs prepared *ex situ*. This second approach can take advantage of the tremendous developments in controlling the growth of monodisperse and highly crystalline quantum dots of diverse semiconductor materials.[21] However, the *ex situ* growth approach requires, in a second step, facile methods to incorporate the QDs onto the electrodes to achieve effective QD−electrode junctions that would promote charge separation while minimizing surface trapping and hence losses.

Most commonly, a linker-based approach was used, in which the mesoporous TiO_2 electrodes were coated by bifunctional molecular linkers, followed by immersing the electrode in a solution of QDs for deposition. This *ex situ* fabrication method suffers from two main drawbacks; first, due to the high aspect *ratio* porosity of the electrode and lack of clear driving force for deposition, long deposition times (24−96 h) are needed to achieve reasonable coverage and optical density of the absorbing sensitizer. Second, mostly poor photoelectric responses could be achieved, likely because of the presence of a barrier for electron injection introduced by the linker molecule.[4,8]

An additional method for *ex situ* deposition of QDs to TiO_2 electrodes was suggested by Bisquert,[5] Gomez,[22] and coworkers using direct adsorption (DA). The principle of this method includes solvent/nonsolvent precipitation of QDs from the solution onto the mesoporous electrodes. However, this precipitation process cannot

*Address correspondence to banin@chem.ch.huji.ac.il, zabana@mail.biu.ac.il.

Received for review May 13, 2010 and accepted September 20, 2010.

Published online September 24, 2010. 10.1021/nn1018208

be easily controlled due to the tendency of the QDs to agglomerate in solution, leading to uneven and polydisperse coverage by aggregates.

Here we introduce a modified approach for *ex situ* quantum dot sensitized solar cell fabrication, employing electrophoretic deposition of semiconductor QDs into mesoporous TiO_2. Electrophoretic deposition (EPD) was previously employed to deposit semiconductor,[23−29] metallic,[30−32] and insulating[33,34] nanoparticles on conductive substrates and polymers.[32,35−37] Herman and co-workers have reported depositions of CdSe QDs adhering strongly both on negative and positive electrodes.[26,28,38−45] First steps in applying electrophoretic deposition for solar-cell fabrication were also reported.[33,46] Rosenthal[47] and co-workers have fabricated photovoltaic cells by EPD of CdSe nanocrystals on flat TiO_2, yielding low conversion efficiencies. Kamat and co-workers[48,49] have used EPD of carbon nanotubes−CdSe NPs composites and C60−CdSe NPs composites to prepare solar cells, yielding also low efficiencies. So far, the early efforts did not provide a high efficiency and were not applied to deposit CdSe QDs on mesoporous TiO_2-based solar cells.

Our work shows that the EPD on the TiO_2 electrodes indeed provides a driving force leading to highly effective QD deposition on the mesoporous TiO_2 surface. This allows us to shorten the fabrication time considerably, and high coverage was achieved already after 2 h. Detailed microscopic and chemical analysis provides proof for penetration of the QDs through the depth of the TiO_2 layer, reflecting the effectiveness of the EPD method in this case. Moreover, the photovoltaic characteristics of the devices were improved greatly, especially after postdeposition surface treatment with ZnS, reaching values that approach those reported for *in situ* prepared QDSSCs. This is indicative of the good connectivity between the QDs and the TiO_2 enabled by this EPD preparation method. Additionally, the size dependence of the photovoltaic characteristics was investigated, and QDs with larger diameters showed improved performance, unlike in previous reports employing a linker strategy. The EPD method can be easily applied generally to deposit QD sensitizers NPs of diverse semiconductor and of different morphologies as we also demonstrate for deposition of quantum rod semiconductors.

RESULTS AND DISCUSSION

CdSe quantum dots of diameters ranging between 2.5−5.5 nm were synthesized using high temperature pyrolysis of organometallic precursors in a coordinating solvent as in known literature procedures. The QDs are overcoated by a mixture of tributylphosphine (TBP) and trioctylphosphineoxide (TOPO).[50] Mesoporous TiO_2 layers were deposited by EPD on fluorinated tin oxide (FTO) transparent electrodes, followed by hydraulic

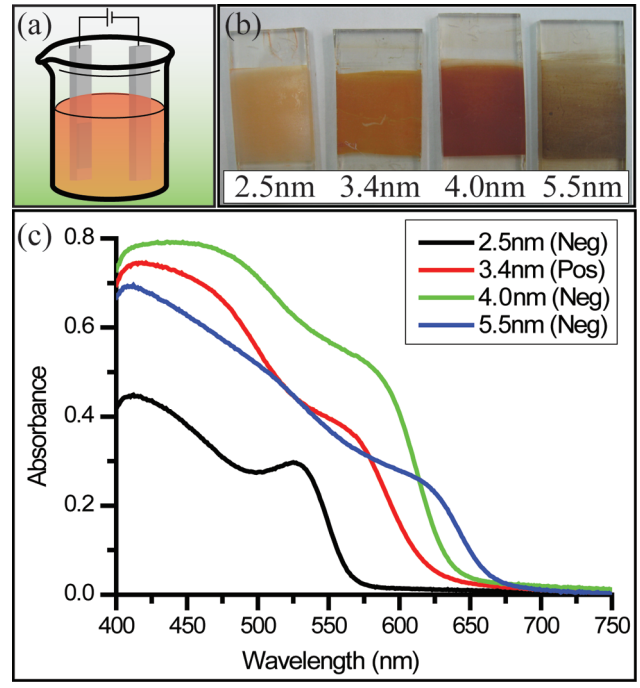

Figure 1. (a) Illustration of the EPD system; (b) images of QDs-TiO_2 electrodes after 2 h of EPD. (c) Absorbance of QDs on the TiO_2 electrodes: (black line) 2.5, (red) 3.4, (green) 4, and (blue) 5.5 nm QDs. For the simplification of data observed, we present the more efficient electrodes after ZnS treatment from each pair of electrodes (negative and positive) per QDs; the full data is presented in the Supporting Information, Figure S2.

pressing and high temperature sintering, reaching thicknesses up to 5 μm. For EPD of the QDs, pairs of mesoporous TiO_2 electrodes were immersed in toluene solutions of the nanoparticles, with typical concentrations of 10^{-7} M, and a DC voltage of 200 V was applied for 2 h (see Figure 1a). A coloring of the electrodes was clearly visible as seen in Figure 1b, indicative of QD deposition, unlike when the electrodes were immersed in toluene with no voltage applied (Supporting Information, Figure S3). The absorbance of the electrodes was measured using an integrating sphere (Figure 1c and Supporting Information, Figure S1). Deposition on both the positive and the negative electrodes was seen. This is indicative of QDs with either negative or positive excess charges, likely attributed to the surface ligands, and consistent with earlier studies of deposition onto conductive electrodes.[39,40] Some broadening of the QD absorption features occurred upon deposition compared with the solution absorbance, and the band gap of the QDs on the electrodes showed only slight changes (Supporting Information, Figure S1).

Chemical analysis performed on cross sections of the electrodes using energy dispersive X-ray spectroscopy (EDS) in a high resolution scanning electron microscope (HRSEM) is presented in Figure 2 for the negative 4.0 nm electrode. The Ti/Cd atomic ratio is nearly constant throughout the entire TiO_2 cross-section as was also seen for other QD sizes (Supporting Information, Figure S4). Electron flight simulation, Monte Carlo model-

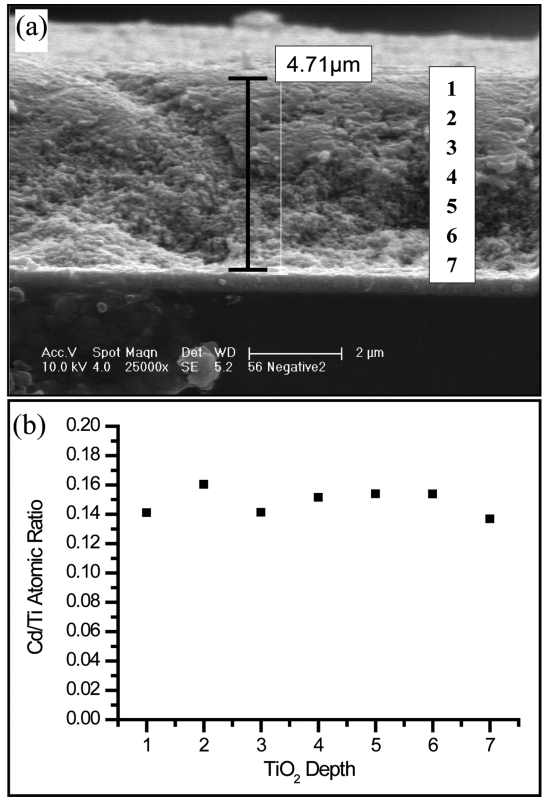

Figure 2. (a) HRSEM image of a cross-section of TiO_2 with 4 nm QDs; numbers indicate the points on the TiO_2 where EDS analysis was made. (b) Cd−Ti ratio measured at different cross-section heights of the TiO_2 using EDS analysis.

ing, performed in order to determine the EDS spot size made using the HRSEM on the TiO_2 cross section, has revealed a spot size of 1.2 µm; therefore, some overlap is seen between the close spots.

Chemical analysis of the electrode at significantly higher resolution was then done by fabrication of lamella cross section of the 4.0 nm QDs TiO_2 negative electrode using a focused ion beam (FIB). The lamella was characterized using line scan energy dispersive X-ray spectroscopy (EDS) in a high resolution transmission electron microscope (HRTEM) operated at 200 kV (inset of Figure 3a). The line scan shows Ti (green), Cd (red), and Se (white) intensities acquired by the detector. The dispersion of X-ray electrons emitted from the lamella, calculated by electron flight simulations, was found to be <40 nm; therefore, the signals recorded from the EDS line scan are in the same range of the granulation of the P-25 TiO_2 and follow the pattern of the cross section. Looking at the normalized signals of Ti and Cd, a similar trend is seen between the signals throughout the TiO_2 cross section (Figure 3a) which indicates homogeneous coverage of QDs on the TiO_2 particles, all the way down to the FTO substrate. The ratio between Cd and Ti atom signals recorded from the scan was calculated (Figure 3b) and does not show a gradient trend throughout the cross section. The average signal is 0.16, closely similar to the ratio recorded using the EDS analysis made using the SEM. Additional analysis along the width of the lamella cross section, at three different heights, is presented in Supporting Information, Figure S5. The atomic ratio between Cd and Ti does not show a gradient trend, which also indicates that the CdSe coverage along the mesoporous TiO_2 is closely similar. Both EDS SEM and EDS HRTEM have determined effective penetration and homogeneous deposition of the QDs throughout the mesoporous network down to the FTO substrate, taking place in a fast time scale of only 2 h.

To further demonstrate the versatility of our method we have also deposited by the same method 20 × 4 nm CdSe quantum rods (QRs) into mesoporous TiO_2 electrodes and analyzed a lamella cross section of the electrode using EDS line scan in the HRTEM (Supporting Information, Figure S6). The Ti to Cd atom ratio along the lamella cross section changes only slightly. The average ratio between Cd and Ti atoms is 0.09, lower compared to QDs, likely because of the longer axis of the rod. This result suggests that electrophoretic deposition of different morphologies of nanoparticles

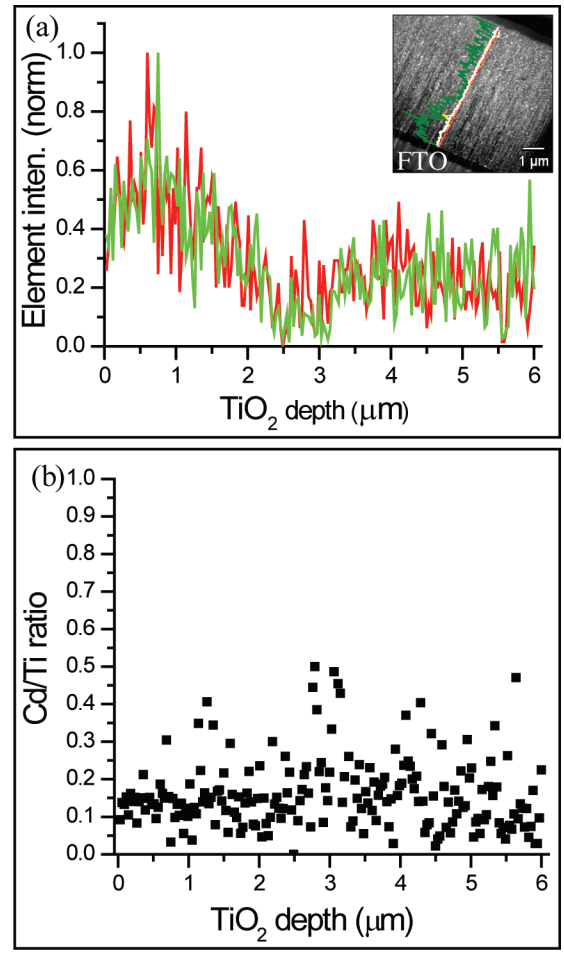

Figure 3. (a) Normalized Ti (green) and Cd (red) element signal intensity. Inset, STEM EDS line scan of a lamella cross section of TiO_2 with negative 4.0 nm QDs electrode. The analysis was made from the FTO toward the top of the TiO_2. Colored lines indicate intensities of elements, Ti (green), Cd (red), and Se (white). (b) Cd−Ti atom ratio, not normalized, (black dots) measured from the line scan.

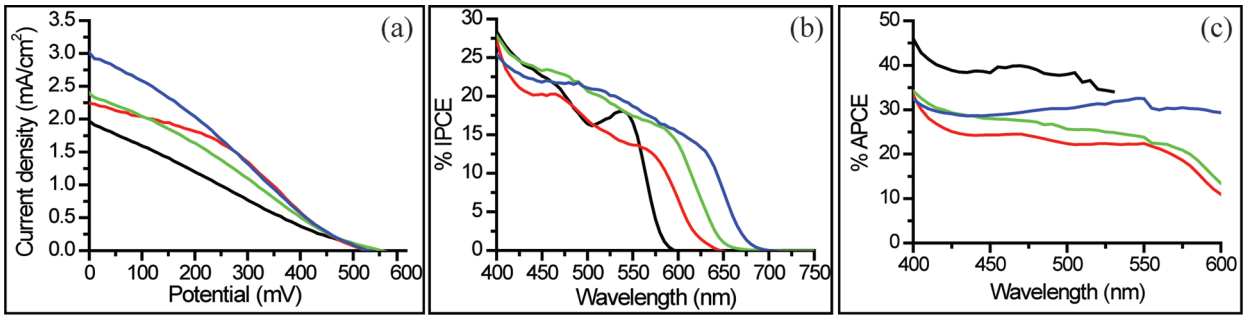

Figure 4. (a) Current−voltage characteristics of illuminated solar cells after deposition of different sizes of QDs on TiO_2 under 1 sun AM 1.5 illuminations: (black line) 2.5, (red) 3.4, (green) 4, and (blue) 5.5 nm. (b) Incident photon to charge efficiency (IPCE) of different sizes of QDs on TiO_2 electrodes. (c) Absorbed photon to charge efficiency (APCE) of different sizes of QDs on TiO_2 electrodes.

(as QDs and QRs) into mesoporous TiO_2 can also be practiced with almost constant coverage.

BET measurements done on the TiO_2 particles after sintering yielded a specific surface area of 49 m^2/g which is in agreement with literature values.[51,52] Deriving the area that would be covered by the nanoparticles on the electrodes using absorbance measurements have revealed less than 0.2 monolayer of QDs coverage (detailed calculations in the Supporting Information and Table S1).

Next, QDSSC devices were prepared by depositing 20 μL of 1 M polysulfide electrolyte on the electrode and closing the cell with a Pt counter-electrode using 50 μm thick Teflon spacers. The photovoltaic performance is shown in Figure 4, and the main parameters are presented in Table 1, comparing the four different QD sizes (2.5, 3.4, 4, and 5.5 nm). The current−voltage ($I-V$) characteristics in Figure 4a show for all sizes an open circuit voltage, V_{OC} of ~550 mV, while the short-circuit current, J_{SC}, varies slightly between 2 and 3 mA/cm^2. The extracted overall efficiencies under AM1.5 1 sun illumination conditions range between 0.3% and 0.4%. Notably, the 3.4, 4, and 5.5 nm electrodes all show similar efficiencies of ~0.4%. This is a remarkable result in light of earlier work studying the electron transfer in linker-based QDSSC electrodes, which showed exponential decrease of the transfer rate with increasing size varying by 3 orders of magnitude between 2.4 nm CdSe QDs to 7.5 nm QDs.[8,9] This was correlated with the downward shift of the CdSe $1S_e$ conduction level with increasing QD size which reduces significantly the energetic driving force for the charge transfer to the TiO_2. In contrast, for our EPD prepared QDSSC, the incident photon to electron conversion efficiencies for the four sizes presented in Figure 4b, shows similar behavior for all sizes, with the onset increasing to longer wavelengths for the larger sizes, in correspondence with their smaller band gap energies. To examine more carefully the size dependence (or in fact its absence in this case), we calculated the APCE (absorbed photon to electron conversion efficiency) by dividing the %IPCE by the absorbance spectrum (Figure 4c). This takes out the effect of varying optical densities of the different electrodes. Clearly, the values do not show a systematic size-dependence, and are 30−40% for all the electrodes, within the experimental variations (Supporting Information, Figure S9). Moreover, the larger QDs do not show decreased APCE or efficiency values.

For further improvement of the cell performance we applied to all the electrodes a postdeposition treatment of coating by a thin layer of ZnS as previously reported. Briefly, electrodes were dipped for two cycles of 1 min in 0.1 M aqueous solutions of zinc acetate and sodium sulfide.[5,16,53] The coating with ZnS can improve the passivation of the QDs, reducing undesired surface trapping processes, and may also assist through coating of the electrode. Figure 5 and Table 2 show the photovoltaic characteristics of the electrodes after the ZnS treatment. The performance dramatically increased for all the electrodes, with maximal enhancement achieved in this set for the 4 nm QD electrode (see inset for comparisons of the curves before and after ZnS treatment). J_{SC} increased by a factor of 3.5 to 9 mA/cm^2, and the fill factor increased from 26% to 35%. Overall, the efficiency of this cell increased from 0.4% to 1.7% after the ZnS treatment; to our best knowledge a record value for *ex situ* prepared QDSSCs with CdSe nanocrystals.

The IPCE measurements also show significant improvements after the ZnS treatment, for all the electrodes. The 4 nm cell has maximal IPCE of 70% at 400 nm and 50% at the excitonic peak (624 nm). The APCE values increase as well, up to 80% and even higher for the 4 nm electrode indicating that most of the QDs indeed contribute to the total photocurrent, and that most absorbed photons lead to charge injection.

The superior performance of the QDSSCs prepared by our EPD approach is demonstrated also by studying

TABLE 1. Summary of $I-V$ Photovoltaic Characteristic of QDs on TiO_2

sample	V_{oc} (mV)	J_{sc} (mA/cm^2)	FF (%)	efficiency (%)
2.5 nm neg	554	2.0	23	0.3
3.4 nm pos	524	2.3	35	0.4
4.0 nm neg	554	2.7	26	0.4
5.5 nm neg	524	3.0	27	0.4

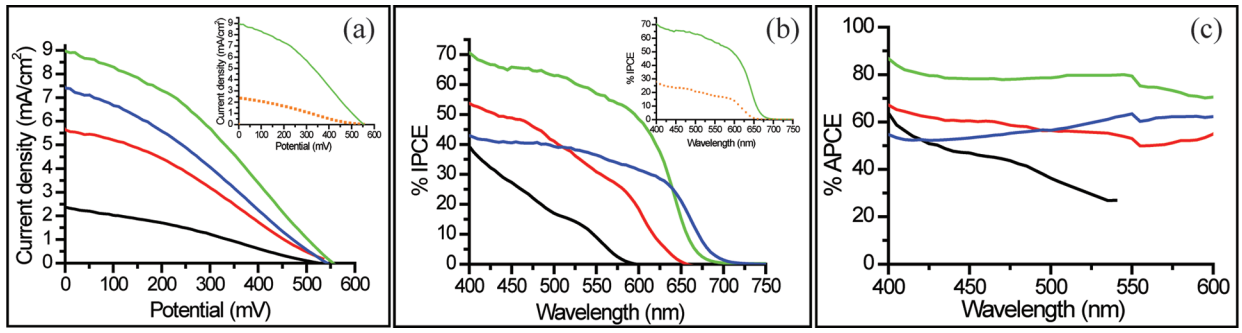

Figure 5. (a) Current−voltage characteristics of illuminated solar cells of different sizes of QDs after ZnS treatment on TiO_2, illuminated at intensity of 1 sun AM 1.5: (black) 2.5, (red) 3.4, (green) 4, and (blue) 5.5 nm. Inset, 4 nm QDs before ZnS treatment (orange) and after ZnS treatment (green). (b) Incident photon to charge efficiency (IPCE) of different sizes of QDs on TiO_2 electrodes; inset, 4 nm QDs before ZnS treatment (orange) and after ZnS treatment (green). (c) Absorbed photon to charge efficiency (APCE) of different sizes of QDs on TiO_2 electrodes.

the dependence of the photocurrent on illumination intensity and on recurring dark-light exposures. Figure 6 presents J_{SC} as a function of the illumination intensity for the 3.4 nm QDSSC starting from the highest light intensity which was decreased stepwise using neutral density filters. A linear behavior over the entire intensity range is observed indicating stable performance even at higher intensities measured, up to 1 sun. Moreover, immediate and stable photocurrent response following light-on is seen (Supporting Information, Figure S13). In contrast, similar measurements on QDSSCs prepared by the SILAR and linker approaches have shown sublinear dependence of the photocurrent on the illumination intensity, and under illumination intensities higher than 0.5 sun the immediate photocurrent decreased until saturation.[8,19,54] The same problems were actually also observed for *in situ* QDSSCs but remarkably, our EPD prepared QDSSCs show stable performance indicative of efficient charge injection. This, accompanied by the lack of clear size dependence, implies a good coupling for the EPD deposited QDs with the TiO_2.[53]

Summarizing, *ex situ* QDSSC fabrication employing electrophoretic deposition of QDs and QRs was developed. After only 2 h of deposition, good electrode coverage was achieved, with close to uniform deposition of the CdSe QDs and QRs throughout the entire mesoporous TiO_2 layer. Therefore, the EPD approach provides a facile and reproducible route for QDSSC preparation. The EPD prepared QDSSCs were then subjected to the ZnS surface treatment, yielding cells with exceptional photovoltaic performance, en-par with values obtained for well established *in situ* prepared QDSSC cells. The highest efficiency was observed so far for 4 nm QDSSC, reaching levels of 1.7% at 1 sun and showing stable linear performance under varying light intensities. Moreover, we do not observe a significant dependence on QD size, for diameters up to 5.5 nm, unlike linker-based electrodes which showed an exponential decrease of the electron injection rate for increased QD sizes. The EPD approach for QDSSC fabrication can be easily applied to high quality *ex situ* grown quantum dots of diverse materials, as demonstrated here for larger quantum rods, which will be further examined as sensitizers. We thus envision its importance in assisting to benchmark and continue improvements of the performance of QDs sensitized solar cell devices.

TABLE 2. Summary of *I*−*V* Photovoltaic Properties of QDs on TiO_2, after ZnS Treatment

sample	V_{oc} (mV)	J_{sc} (mA/cm²)	FF (%)	efficiency (%)
2.5 nm neg	524	2.4	32	0.4
3.4 nm pos	554	5.6	31	1.0
4.0 nm neg	554	9.0	35	1.7
5.5 nm neg	544	7.4	32	1.3

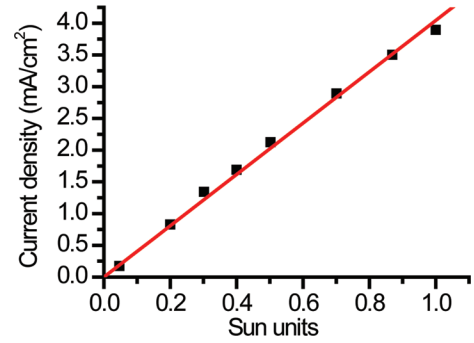

Figure 6. Current density as a function of light intensity in sun units for different illumination intensities using ND filters: (i) 1, (ii) 0.87, (iii) 0.70, (iv) 0.50, (v) 0.40, (vi) 0.30, (vii) 0.20, and (viii) 0.05 sun on a 3.4 nm QDs on TiO_2 electrode.

METHODS AND MATERIALS

CdSe QDs Synthesis. CdSe QDs of different diameters were prepared by known literature procedures. In a typical reaction, 4 g of trioctylphosphine oxide (TOPO) (technical, Sigma) was weighed into a 25 mL three-neck flask attached to a shlenk line with Ar flow. A 0.8 g portion of selenium (Sigma) was dissolved in 8 mL of tributylphosphine (TBP) (Aldrich), and this mixture was further mixed with 2 g of $Cd(Me)_2$ (Strem). A 2.5 mL aliquot of the Cd/Se/TBP solution was mixed with 6 g of TBP and injected into the flask at 360 °C. After the nucleation, the temperature was

reduced to 270 °C for the growth stage. The growth was monitored by measuring the absorbance spectrum of aliquots extracted from the reaction solution. For the larger diameter cores, 0.2 mL of the Cd/Se/TBP precursor solutions was added. The synthesis was stopped after reaching the wanted size by cooling the solution to room temperature. For the EPD the QDs were separated from excess TOPO/TBP by dissolving the QDs in toluene and precipitating with methanol three times using centrifugation at 6000 rpm.

TiO_2 Electrode Preparation. Mesoporous TiO_2 films were prepared by electrophoretic deposition (EPD) of Degussa P25 particles with an average diameter of 25 nm onto fluorine-doped tin oxide (FTO) covered glass substrates (Pilkington TEC 8) with 8 Ω^2 sheet resistance. Films were deposited in four consecutive cycles for 30 s at a constant current density of 0.4 mA/cm^2, and dried at 120 °C for 5 min in between the cycles. Following the EPD process all the electrodes were dried in air at 150 °C for 30 min, pressed under 800 kg/cm^2 using a hydraulic press, and sintered at 550 °C for 1 h.

Electrophoretic Deposition of the QDs on the TiO_2 Electrodes. QDs were redispersed in toluene (tech.), with typical concentrations of 10^{-7} M. Two TiO_2 FTO electrodes were immersed in the QDs solution, and a voltage of 0.2 kV was applied for 2 h. To wash off unbound QDs after the EPD process, the electrodes were rinsed several times with toluene.

Absorbance of Solution and Electrodes. The QDs were dissolved in toluene in different optical densities, as seen in Supporting Information, Figure S1, and absorbance spectra were measured using a Jasco UV−vis spectrophotometer. The QDs-TiO_2 electrodes were measured using a Varian spectrophotometer equipped with an integrating sphere.

Lamella Fabrication. Lamella cross section of the TiO_2-CdSe electrode was done using a Helios 600, dual beam SEM and FIB instrument. The electrode was cut out of and connected to a corner of a TEM grid for HRTEM analysis. The thickness of the lamella was ~50 nm.

SEM Analysis. SEM-EDS analysis was performed using an FEI Sirion high resolution SEM system operated at 10−15 kV accelerating voltage. Measurements were taken at equal spacing from the FTO glass surface along a freshly cleaved cross-section of the TiO_2. The samples were coated with a thin layer of Au and Pd by sputtering in order overcome charging effects. We have followed the peaks of Cd−L and Ti−K spectrum in order to find the ratio between Cd and Ti at these locations.

HRTEM Analysis. TEM imaging and line scan analysis of the lamella was performed using high resolution transmission electron microscope, Jeol JEM-2100, operated at 200 kV accelerating voltage.

Electron Flight Simulation. Monte Carlo modeling for the analysis of the resolution of the EDS cross section analysis was carried out using an electron flight simulator, version 3.1-E. (For HRSEM 10−15 kV was set with 50% porosity of TiO_2, with an Au−Pd thin film of 8 nm, for HRTEM analysis 200 kV was set, with 50% porosity of TiO_2 with 50 nm thickness).

BET Measurement. BET measurement was carried out using Micromeritics ASAP 2020 Surface Area and Porosity with Analyzer Software V3.00. A 1 g portion of P-25 TiO_2 was prepared as described above and loaded to the BET instrument for measurement.

***I*−*V* IPCE Measurement.** Photocurrent−voltage characteristics were performed with an Eco-Chemie potentiostat using a scan rate of 10 mV/s. A 250 W xenon arc lamp (Oriel) calibrated to 100 mW/cm^2 (AM 1.5 spectrum) served as a light source. The illuminated area of the cell was set to 0.64 cm^2 using an aperture. 1 M Na_2S, 0.1 M sulfur, and 0.1 M KOH (all from Sigma) solution served as the electrolyte. A sputtered Pt-coated FTO glass was used as a counter-electrode. Measuring photocurrent *versus* time and illumination was made by manual shuttering and exchanging the filters.

Acknowledgment. We wish to thank Dr. Inna Popov and Mrs. Evgenia Blayvas for assistance with the Monte Carlo simulations and in SEM imaging made at the Harvey M. Krueger family center for nanoscience and nanotechnology. Dr. Yafit Fleger assisted in FIB and lamella fabrication. Dr. Judith Grinblat and Dr. Ilana Perelshtein, in HRTEM analysis at Bar Ilan University. Mrs. Hadas Friedman is thanked for BET measurements. This research was funded by the Israel Ministry of Industry and Trade under the SES (Solar Energy Solutions) MAGNET program. U.B. thanks the Alfred and Erica Larisch Memorial Chair in Solar Energy.

Supporting Information Available: Additional analyses including positive and negative counterelectrodes absorbance, EDS of HRSEM and HRTEM, BET, *I*−*V*, IPCE, and APCE analyses. This material is available free of charge *via* the Internet at http://pubs.acs.org.

REFERENCES AND NOTES

1. Zaban, A.; Micic, O. I.; Gregg, B. A.; Nozik, A. J. Photosensitization of Nanoporous TiO_2 Electrodes with InP Quantum Dots. *Langmuir* **1998**, *14*, 3153–3156.
2. Nozik, A. J. Quantum Dot Solar Cells. *Phys. E* **2002**, *14*, 115–120.
3. Kamat, P. V. Quantum Dot Solar Cells. Semiconductor Nanocrystals as Light Harvesters. *J. Phys. Chem. C* **2008**, *112*, 18737–18753.
4. Mora-Sero, I.; Gimenez, S.; Moehl, T.; Fabregat-Santiago, F.; Lana-Villareal, T.; Gomez, R.; Bisquert, J. Factors Determining the Photovoltaic Performance of a CdSe Quantum Dot Sensitized Solar Cell: The Role of the Linker Molecule and of the Counter Electrode. *Nanotechnology* **2008**, *19*, 424007.
5. Gimenez, S.; Mora-Sero, I.; Macor, L.; Guijarro, N.; Lana-Villarreal, T.; Gomez, R.; Diguna, L. J.; Shen, Q.; Toyoda, T.; Bisquert, J. Improving the Performance of Colloidal Quantum-Dot-Sensitized Solar Cells. *Nanotechnology* **2009**, *20*, 295204.
6. Gao, X. F.; Li, H. B.; Sun, W. T.; Chen, Q.; Tang, F. Q.; Peng, L. M. CdTe Quantum Dots-Sensitized TiO_2 Nanotube Array Photoelectrodes. *J. Phys. Chem. C.* **2009**, *113*, 7531–7535.
7. Lee, H.; Leventis, H. C.; Moon, S. J.; Chen, P.; Ito, S.; Haque, S. A.; Torres, T.; Nuesch, F.; Geiger, T.; Zakeeruddin, S. M.; *et al.* PbS and US Quantum Dot-Sensitized Solid-State Solar Cells: Old Concepts, New Results. *Adv. Funct. Mater.* **2009**, *19*, 2735–2742.
8. Robel, I.; Subramanian, V.; Kuno, M.; Kamat, P. V. Quantum Dot Solar Cells. Harvesting Light Energy with CdSe Nanocrystals Molecularly Linked to Mesoscopic TiO_2 Films. *J. Am. Chem. Soc.* **2006**, *128*, 2385–2393.
9. Kongkanand, A.; Tvrdy, K.; Takechi, K.; Kuno, M.; Kamat, P. V. Quantum Dot Solar Cells. Tuning Photoresponse through Size and Shape Control of CdSe-TiO_2 Architecture. *J. Am. Chem. Soc.* **2008**, *130*, 4007–4015.
10. Ruhle, S.; Shalom, M.; Zaban, A. Quantum-Dot-Sensitized Solar Cells. *ChemPhysChem* **2010**, *11*, 2290–2304.
11. Lee, Y. L.; Huang, B. M.; Chien, H. T. Highly Efficient CdSe-Sensitized TiO_2 Photoelectrode for Quantum-Dot-Sensitized Solar Cell Applications. *Chem. Mater.* **2008**, *20*, 6903–6905.
12. Nasr, C.; Hotchandani, S.; Kim, W. Y.; Schmehl, R. H.; Kamat, P. V. Photoelectrochemistry of Composite Semiconductor Thin Films. Photosensitization of SnO_2/CdS Coupled Nanocrystallites with a Ruthenium Polypyridyl Complex. *J. Phys. Chem B* **1997**, *101*, 7480–7487.
13. Niitsoo, O.; Sarkar, S. K.; Pejoux, C.; Ruhle, S.; Cahen, D.; Hodes, G. Chemical Bath Deposited CdS/CdSe-Sensitized Porous TiO_2 Solar Cells. *J. Photochem. Photobiol. A* **2006**, *181*, 306–313.
14. Gorer, S.; Hodes, G. Quantum-Size Effects in the Study of Chemical Solution Deposition Mechanisms of Semiconductor-Films. *J. Phys. Chem.* **1994**, *98*, 5338–5346.
15. Shalom, M.; Dor, S.; Ruhle, S.; Grinis, L.; Zaban, A. Core/CdS Quantum Dot/Shell Mesoporous Solar Cells with Improved Stability and Efficiency Using an Amorphous TiO_2 Coating. *J. Phys. Chem. C* **2009**, *113*, 3895–3898.
16. Diguna, L. J.; Shen, Q.; Kobayashi, J.; Toyoda, T. High Efficiency of CdSe Quantum-Dot-Sensitized TiO_2 Inverse Opal Solar Cells. *Appl. Phys. Lett.* **2007**, *91*, 023116.
17. Shalom, M.; Ruhle, S.; Hod, I.; Yahav, S.; Zaban, A. Energy Level Alignment in CdS Quantum Dot Sensitized Solar

Cells Using Molecular Dipoles. *J. Am. Chem. Soc.* **2009**, *131*, 9876–9877.
18. Shalom, M.; Albero, J.; Tachan, Z.; Martinez Ferrero, E.; Zaban, A.; Palomares, E. Quantum Dot Dye Bilayer-Sensitized Solar Cells: Breaking the Limits Imposed by the Low Absorbance of Dye Monolayers. *J. Phys. Chem. Lett.* **2010**, *1*, 1134–1138.
19. Lee, H.; Wang, M. K.; Chen, P.; Gamelin, D. R.; Zakeeruddin, S. M.; Gratzel, M.; Nazeeruddin, M. K. Efficient CdSe Quantum Dot-Sensitized Solar Cells Prepared by an Improved Successive Ionic Layer Adsorption and Reaction Process. *Nano Lett.* **2009**, *9*, 4221–4227.
20. Chang, C. H.; Lee, Y. L. Chemical Bath Deposition of CdS Quantum Dots onto Mesoscopic TiO_2 Films for Application in Quantum-Dot-Sensitized Solar Cells. *Appl. Phys. Lett.* **2007**, *91*, 053503.
21. Bang, J. H.; Kamat, P. V. Quantum Dot Sensitized Solar Cells. A Tale of Two Semiconductor Nanocrystals: CdSe and CdTe. *ACS Nano* **2009**, *3*, 1467–1476.
22. Guijarro, N.; Lana-Villarreal, T.; Mora-Sero, I.; Bisquert, J.; Gomez, R. CdSe Quantum Dot-Sensitized TiO_2 Electrodes: Effect of Quantum Dot Coverage and Mode of Attachment. *J. Phys. Chem. C* **2009**, *113*, 4208–4214.
23. Mahajan, S. V.; Cho, J.; Shaffer, M. S. P.; Boccaccini, A. R.; Dickerson, J. H. Electrophoretic Deposition and Characterization of Eu_2O_3 Nanocrystal−Carbon Nanotube Heterostructures. *J. Eur. Ceram. Soc.* **2010**, *30*, 1145–1150.
24. Mahajan, S. V.; Dickerson, J. H. Dielectric Properties of Colloidal Gd_2O_3 Nanocrystal Films Fabricated *via* Electrophoretic Deposition. *Appl. Phys. Lett.* **2010**, *96*, 113105.
25. Mahajan, S. V.; Dickerson, J. H. Understanding the Growth of Eu_2O_3 Nanocrystal Films made *via* Electrophoretic Deposition. *Nanotechnology* **2010**, 21.
26. Mahajan, S. V.; Hasan, S. A.; Cho, J.; Shaffer, M. S. P.; Boccaccini, A. R.; Dickerson, J. H. Carbon Nanotube−Nanocrystal Heterostructures Fabricated by Electrophoretic Deposition. *Nanotechnology* **2008**, *19*, 145704.
27. Ameen, S.; Akhtar, M. S.; Ansari, S. G.; Yang, O. B.; Shin, H. S. Electrophoretically Deposited Polyaniline/ZnO Nanoparticles for P−N Heterostructure Diodes. *Superlattices Microstruct.* **2009**, *46*, 872–880.
28. Dogan, A.; Gunkaya, G.; Suvaci, E.; Niederberger, M. Electrophoretic Deposition of Nanocrystalline $BaTiO_3$ in Ethanol Medium. In *Electrophoretic Deposition: Fundamentals and Applications II*; Boccaccini, A. R., VanderBiest, O., Clasen, R., Eds.; The Electrochemical Society: Pennington, NJ, 2006; *Vol. 314*, pp 133−139.
29. Wong, M. E.; Searson, P. C. ZnO Quantum Particle Thin Films Fabricated by Electrophoretic Deposition. *Appl. Phys. Lett.* **1999**, *74*, 2939–2941.
30. Giersig, M.; Mulvaney, P. Formation of Ordered Two-Dimensional Gold Colloid Lattices by Electrophoretic Deposition. *J. Phys. Chem.* **1993**, *97*, 6334–6336.
31. Teranishi, T.; Hosoe, M.; Tanaka, T.; Miyake, M. Size Control of Monodispersed Pt Nanoparticles and Their 2D Organization by Electrophoretic Deposition. *J. Phys. Chem B* **1999**, *103*, 3818–3827.
32. Patel, M. N.; Williams, R. D.; May, R. A.; Uchida, H.; Stevenson, K. J.; Johnston, K. P. Electrophoretic Deposition of Au Nanocrystals inside Perpendicular Mesochannels of TiO_2. *Chem. Mater.* **2008**, *20*, 6029–6040.
33. Grinis, L.; Dor, S.; Ofir, A.; Zaban, A. Electrophoretic Deposition and Compression of Titania Nanoparticle Films for Dye-Sensitized Solar Cells. *J. Photochem. Photobiol. A* **2008**, *198*, 52–59.
34. Ferrari, B.; Bartret, A.; Baudin, C. Sandwich Materials Formed by Thick Alumina Tapes and Thin-Layered Alumina−Aluminium Titanate Structures Shaped by EPD. *J. Eur. Ceram. Soc.* **2009**, *29*, 1083–1092.
35. Vidotti, M.; de Torresi, S. I. C. Electrostatic Layer-by-Layer and Electrophoretic Depositions as Methods for Electrochromic Nanoparticle Immobilization. *Electrochim. Acta* **2009**, *54*, 2800–2804.
36. Gao, M. Y.; Sun, J. Q.; Dulkeith, E.; Gaponik, N.; Lemmer, U.; Feldmann, J. Lateral Patterning of CdTe Nanocrystal Films by the Electric Field Directed Layer-by-Layer Assembly Method. *Langmuir* **2002**, *18*, 4098–4102.
37. Sun, J. Q.; Gao, M. Y.; Feldmann, J. Electric Field Directed Layer-by-Layer Assembly of Highly Fluorescent CdTe Nanoparticles. *J. Nanosci. Nanotechnol.* **2001**, *1*, 133–136.
38. Islam, M. A.; Herman, I. P. Electrodeposition of Patterned CdSe Nanocrystal Films Using Thermally Charged Nanocrystals. *Appl. Phys. Lett.* **2002**, *80*, 3823–3825.
39. Islam, M. A.; Xia, Y. Q.; Telesca, D. A.; Steigerwald, M. L.; Herman, I. P. Controlled Electrophoretic Deposition of Smooth and Robust Films of CdSe Nanocrystals. *Chem. Mater.* **2004**, *16*, 49–54.
40. Jia, S.; Banerjee, S.; Herman, I. P. Mechanism of the Electrophoretic Deposition of CdSe Nanocrystal Films: Influence of the Nanocrystal Surface and Charge. *J. Phys. Chem. C* **2008**, *112*, 162–171.
41. Islam, M. A.; Xia, Y. Q.; Steigerwald, M. L.; Yin, M.; Liu, Z.; O'Brien, S.; Levicky, R.; Herman, I. P. Addition, Suppression, and Inhibition in the Electrophoretic Deposition of Nanocrystal Mixture Films for CdSe Nanocrystals with Gamma-Fe_2O_3 and Au Nanocrystals. *Nano Lett.* **2003**, *3*, 1603–1606.
42. Vigneashwari, B.; Ravichandran, V.; Parameswaran, P.; Dash, S.; Tyagi, A. K. Nanostructure Assembly of Indium Sulphide Quantum Dots and Their Characterization. *J. Nanosci. Nanotechnol.* **2008**, *8*, 689–694.
43. Kooij, E. S.; Brouwer, E. A. M.; Poelserna, B. Electric Field Assisted Nanocolloidal Gold Deposition. *J. Electroanal. Chem.* **2007**, *611*, 208–216.
44. Xiong, X. G.; Makaram, P.; Busnaina, A.; Bakhtari, K.; Somu, S.; McGruer, N.; Park, J. Large Scale Directed Assembly of Nanoparticles Using Nanotrench Templates. *Appl. Phys. Lett.* **2006**, *89*, 193108.
45. Zhang, Q. L.; Xu, T.; Butterfield, D.; Misner, M. J.; Ryu, D. Y.; Emrick, T.; Russell, T. P. Controlled Placement of CdSe Nanoparticles in Diblock Copolymer Templates by Electrophoretic Deposition. *Nano Lett.* **2005**, *5*, 357–361.
46. Svrcek, V.; Turkevych, I.; Hara, K.; Kondo, M. Ordered Titanium Dioxide Nanotubes Filled with Photoluminescent Surfactant-free Silicon Nanocrystals. *Nanotechnology* **2010**, *21*, 215203.
47. Smith, N. J.; Emmett, K. J.; Rosenthal, S. J. Photovoltaic Cells Fabricated by Electrophoretic Deposition of CdSe Nanocrystals. *Appl. Phys. Lett.* **2008**, *93*, 043504.
48. Brown, P.; Kamat, P. V. Quantum Dot Solar Cells. Electrophoretic Deposition of CdSe-C-60 Composite Films and Capture of Photogenerated Electrons with nC(60) Cluster Shell. *J. Am. Chem. Soc.* **2008**, *130*, 8890–8891.
49. Farrow, B.; Kamat, P. V. CdSe Quantum Dot Sensitized Solar Cells. Shuttling Electrons Through Stacked Carbon Nanocups. *J. Am. Chem. Soc.* **2009**, *131*, 11124–11131.
50. Peng, X. G.; Wickham, J.; Alivisatos, A. P. Kinetics of II−VI and III−V Colloidal Semiconductor Nanocrystal Growth: "Focusing" of Size Distributions. *J. Am. Chem. Soc.* **1998**, *120*, 5343–5344.
51. Ngamsinlapasathian, S.; Sreethawong, T.; Suzuki, Y.; Yoshikawa, S. Single- and Double-Layered Mesoporous TiO_2/P25 TiO_2 Electrode for Dye-Sensitized Solar Cell. *Sol. Energy Mater. Sol. Cells* **2005**, *86*, 269–282.
52. Yu, J.; Yu, H.; Cheng, B.; Zhou, M.; Zhao, X. Enhanced Photocatalytic Activity of TiO_2 Powder (P25) by Hydrothermal Treatment. *J. Mol.Catal. A* **2006**, *253*, 112–118.
53. Shen, Q.; Kobayashi, J.; Diguna, L. J.; Toyoda, T. Effect of ZnS Coating on the Photovoltaic Properties of CdSe Quantum Dot-Sensitized Solar Cells. *J. Appl. Phys.* **2008**, *103*, 084304.
54. Lee, H. J.; Yum, J. H.; Leventis, H. C.; Zakeeruddin, S. M.; Haque, S. A.; Chen, P.; Seok, S. I.; Grazel, M.; Nazeeruddin, M. K. CdSe Quantum Dot-Sensitized Solar Cells Exceeding Efficiency 1% at Full-Sun Intensity. *J. Phys. Chem. C* **2008**, *112*, 11600–11608.